Journal of Pharmaceutical and Biomedical Analysis xxx (2016) xxx–xxx

Contents lists available at ScienceDirect

Journal of Pharmaceutical and Biomedical Analysis

journal homepage: www.elsevier.com/locate/jpba

Looking into aqueous humor through metabolomics spectacles – exploring its metabolic characteristics in relation to myopia

Cecilia Barbas-Bernardos[a,1], Emily G. Armitage[a,1], Antonia García[a], Salvador Mérida[b], Amparo Navea[b,c], Francisco Bosch-Morell[b,c], Coral Barbas[a,*]

[a] Center for Metabolomics and Bioanalysis (CEMBIO), Faculty of Pharmacy, Universidad CEU San Pablo, Campus Monteprincipe, Boadilla del Monte, 28668 Madrid, Spain
[b] Instituto de Ciencias Biomédicas, Universidad CEU Cardenal Herrera, Avenida del Seminario s/n, Moncada, 46313 Valencia, Spain
[c] FISABIO, Oftalmología Médica, Bifurcación Pío Baroja-General Aviles, S/N, 46015 Valencia, Spain

ARTICLE INFO

Article history:
Received 12 November 2015
Received in revised form 11 March 2016
Accepted 14 March 2016
Available online xxx

Keywords:
Metabolomics
Aqueous humor
Myopia
CE–MS
LC–MS
Fingerprinting

ABSTRACT

Aqueous humor is the transparent fluid found in the anterior chamber of the eye that provides the metabolic requirements to the avascular tissues surrounding it. Despite the fact that metabolomics could be a powerful tool in the characterization of this biofluid and in revealing metabolic signatures of common ocular diseases such as myopia, it has never to our knowledge previously been applied in humans. In this research a novel method for the analysis of aqueous humor is presented to show its application in the characterization of this biofluid using CE–MS. The method was extended to a dual platform method (CE–MS and LC–MS) in order to compare samples from patients with different severities of myopia in order to explore the disease from the metabolic phenotype point of view.

With this method, a profound knowledge of the metabolites present in human aqueous humor has been obtained: over 40 metabolites were reproducibly and simultaneously identified from a low volume of sample by CE–MS, including among others, a vast number of amino acids and derivatives. When this method was extended to study groups of patients with high or low myopia in both CE–MS and LC–MS, it has been possible to identify over 20 significantly different metabolite and lipid signatures that distinguish patients based on the severity of myopia. Among these, the most notable higher abundant metabolites in high myopia were aminooctanoic acid, arginine, citrulline and sphinganine while features of low myopia were aminoundecanoic acid, dihydro-retinoic acid and cysteinylglycine disulfide.

This dual platform approach offered complementarity such that different metabolites were detected in each technique. Together the experiments presented provide a whelm of valuable information about human aqueous humor and myopia, proving the utility of non-targeted metabolomics for the first time in analyzing this type of sample and the metabolic phenotype of this disease.

1. Introduction

Myopia, commonly referred to as short/near-sightedness is the condition that occurs when light entering the eye does not impact in the retina but in front of it, producing focused images when looking at close objects, but generating out of focus images when looking objects that are at a longer distance. An emetrope eye has an axial length and a power combination of the eye lenses (cornea and crystalline lens) that lead to a focused image in the retina. An emetrope eye, therefore, does not need glasses to see well. Myopia is one of the most frequent of the refractive eye defects. It can present in two forms: high myopia where there is an excessive axial length (greater than 26 mm) or low myopia when the axial length is less

Abbreviations: AHA, aqueous humor; CE–MS, Capillary electrophoresis - mass spectrometry; LC–MS, Liquid chromatography - mass spectrometry; D, diopters; IOP, intraocular pressure; QC, Quality control; BGE, background electrolyte; MFE, Molecular Feature Extraction; MT, migration time; RT, retention time; LOESS, Locally estimated scatter-plot smoothing; OPLS-DA, ortho partial least squares - discriminant analysis; VIP, Variable importance projection; ASS, argininosuccinate synthase; SAM, S-adenosylmethionine; SAH, S-adenosylhomocysteine.

* Corresponding author at: CEMBIO, Faculty of Pharmacy, Universidad CEU San Pablo, Campus Monteprincipe, Boadilla del Monte, 28668 Madrid, Spain.
E-mail address: cbarbas@ceu.es (C. Barbas).
[1] Equal amount of work.

http://dx.doi.org/10.1016/j.jpba.2016.03.032
0731-7085/

than 26 mm and there is a mismatch defect of the refractive elements (cornea or lens) that are unable to produce an image focused in the retina. Myopia can be diagnosed in any time of life; patients are normally diagnosed as children (between 8 to 12 years old) and their condition may worsen during adolescence, but myopia can also be diagnosed in adulthood due to visual stress or health conditions such as diabetes [1]. It is known that myopia can be caused by genetic factors; by 2012 almost 30 genes had been identified and associated to myopia [2]. The condition of myopia is considered to be one of the most common human eye diseases, affecting 18.5 % of Asians, 13.2 % of Hispanics, 4.4 % of Caucasians and 6.6 % of African Americans [1]. Since it is very common, the severity of myopia is not considered, although maculopathy, cataract, glaucoma and retinal detachment are some of the complications that myopia can lead to. Nevertheless, high myopia is one of the leading cause of blindness in adulthood in developed countries and is the last step of all these [1]. Therefore myopia is a topic that could lead to many studies in the near future.

Aqueous humor (AH) is a transparent fluid found in the anterior and posterior chamber of the eye. It is secreted by the ciliary epithelium lining the ciliary body. Three mechanisms are involved in aqueous humor formation: diffusion, ultrafiltration and active secretion. Active secretion is the major contributor to aqueous humor formation. The fluid is continuously secreted by the ciliary epithelium and enters first into the posterior chamber; then it travels through the pupil toward the anterior chamber and the trabecular meshwork passively traveling towards the episcleral venous system. The composition of AH depends not only on the nature of its production, but also on the metabolic interchanges that occur within various tissues throughout its intraocular route. It is responsible for the supply of nutrients and oxygen to the avascular tissues through diffusion [3]. The major components of AH are organic and inorganic ions, carbohydrates (glucose), urea, and proteins, oxygen, carbon dioxide and water. As AH is 'a transudate of plasma', provides the amino acids required for the synthesis of lenticular proteins [4]. Besides that, important anti-oxidant substances can also be found in the AH, such as glutathione (derived by diffusion from the blood) and ascorbate (which helps protect against light- induced oxidative damage) and defensive molecules such as immunoglobulins (IgG, IgM and IgA) [3].

AH also removes metabolic waste from the avascular tissues through its continuous formation, moving through the ocular chambers and drainage from the eye to the venous blood. In a healthy eye, the intraocular pressure (IOP) is necessary to inflate the eye as well as to maintain the proper shape and optical properties of the eyeball and AH secretion and outflow are responsible for maintaining IOP. Impaired outflow of AH results in elevation of the IOP, a central principle of glaucoma and its treatment [3].

AH (and more specifically AH in relation to myopia) has previously been studied using proteomics [5–8], but, despite its involvement on the metabolic interchanges throughout its intraocular route, myopia has never to our knowledge been studied through a metabolomics approach in humans. However, AH for different conditions has been previously studied through a metabolomics approach in murine models [9,10]. In this study, an untargeted method using capillary electrophoresis–mass spectrometry (CE–MS) metabolomics has been applied to characterize the profile of AH, chosen due to its applicability within the common platforms for metabolomic analysis to analyze ionic and more polar, water soluble compounds such as amino acids [11] known to be comprised in this type of sample [4]. In addition, the low sample volume consumption characteristic for CE results a great value when working with AH with a limited volume. Following this, AH samples from 36 patients with low (<6 D) myopia and high (≥7 D) myopia were analyzed using the same method in CE–MS and the analysis was extended to include liquid chromatography mass spectrometry (LC–MS), both with accurate mass analyzers in order to gain a wider coverage of metabolites in order to investigate the metabolic alterations with severity of myopia.

1.1. Materials and methods

1.1.1. Experimental design

The study consisted of several experiments. The first was focused on the study of the metabolic profile by CE–MS, whereby six independent preparations were obtained from a sample coming from a healthy individual. For the second experiment, metabolomics was applied to study patients with high or low myopia in order to gain insight into the mechanism of the condition.

1.2. Reagents

All the reagents and standards used were of analytical grade. The dilutions were made with ultrapure water obtained with a MilliQ® system (Millipore, Billerica, MA, USA). The internal standard, methionine sulfone (99%), methanol (MS quality) and formic acid (98%) were from Sigma- Aldrich (Steinheim, Germany). The reference masses used, Purine (121.0509) and HP0921 (922.0098), were obtained from Agilent Technologies (Santa Clara, CA, USA).

1.3. Samples

The samples of AH (50 μL) were kindly provided by the Fundación para el Fomento de la Investigación Sanitaria y Biomédica de la Comunitat Valenciana (FISABI O-Oftalmología Médica) in Valencia (Spain). AH samples were provided for myopic patients: 12 with high myopia (≥26 mm) and 24 with low myopia (< 26,5 mm) and one came from a patient without myopia (for method development). All of the AH samples were extracted during a cataract surgery. All patients provided written informed consent for samples to be taken, and the approval from the ethic committee was obtained for the study.

All samples were diluted with ultrapure water 1:5 (50 μL of sample and 250 μL of water) and were subsequently kept at −80 °C until the day of the experiment. On the day of the experiment, samples were defrosted and homogenized by vortex mixing.

Quality control (QC) samples were prepared by pooling equal volumes of each AH sample and were used in the analysis to observe stability and reproducibility. In both experiments (characterization of the profile and analysis of samples from high and low myopic patients), QCs were injected at the start to reach system stability. In the latter experiment, QCs were also injected every five samples in order to track reproducibility throughout the longer analytical run.

For CE–MS, samples were prepared by mixing 75 μL of the sample (processed as previously described) with 5 μL of internal standard solution resulting in a final concentration by dilution with the AH sample of 0.15 mM methionine sulfone and 0.10 M formic acid. For LC–MS, samples were centrifuged (4 °C, 10 min, 16000 *g*) and the supernatant was analyzed directly.

1.4. Metabolomic platforms

CE–MS analyses were performed on a 7100 capillary electrophoresis (Agilent Technologies) coupled to a 6224 accurate mass TOF MS (Agilent Technologies), equipped with an electrospray ionization (ESI) source. The separation was performed in a capillary with an inner diameter of 50 μm and a total length of 100 cm working in normal polarity. Before each analysis the capillary was conditioned with a background electrolyte (BGE) (0.8 M formic acid solution in 10 % methanol (v/v)) for 5 min at 950 mbar. Sample injections were performed for 50 s at 50 mbar. After the injection

Please cite this article in press as: C. Barbas-Bernardos, et al., Looking into aqueous humor through metabolomics spectacles – exploring its metabolic characteristics in relation to myopia, J. Pharm. Biomed. Anal. (2016), http://dx.doi.org/10.1016/j.jpba.2016.03.032

of each sample the BGE was injected at 100 mbar pressure during 10 s to improve repeatability. The conditions for the separation included an internal pressure of 25 mbar at a voltage of +30 V and with a constant temperature of 20 °C. Analysis time was 30 min. Data were acquired in positive, full scan MS mode, within the range *m/z* 85–1000 at a rate of 1.4 scan/s. The other parameters for the MS were: fragmentor 100 V, skimmer 65 V, octopole 750 V, drying gas temperature 200 °C, flow rate 10 L/min and capillary voltage 3500 V. The sheath liquid used for the detection consisted of 50 % methanol, 50 % ultrapure water, formic acid 1 mM and two reference masses (purine: 121.0509 and HO0921: 922.0098) at a flow rate of 0.6 mL/min (1:100 split). Data acquisition was performed with ChemStation software B.04.03 (Agilent Technologies Santa Clara, CA, USA) and Mass Hunter Workstation Data Analysis B.02.01, (Agilent Technologies) controlled the MS performance.

LC–MS analysis were performed using a UHPLC system (Agilent 1290 Infinity LC System) coupled to a LC-QTOF-MS (6550 iFunnel) system (Agilent Technologies). The UHPLC system consisted of a degasser, two binary pumps and an autosampler (maintained at 4 °C). Samples of AH were injected at 15 μL onto a reverse-phase Zorbax Extend C18 column (2.1 mm x 50 mm, 1.8 μm; Agilent Technologies) maintained at 60 °C. The flow rate was 0.6 mL/min with solvent A composed of water with 0.1% formic acid, and a solvent B composed of acetonitrile with 0.1% formic acid. The chromatographic gradient started at 5% of solvent B up to the first minute, increased to 80% from 1–7 min, then to 100% from 7–11.5 min, and returned to 5% of solvent B from 12–15 min (system re-equilibration) with the analysis time of 15 min. Data were collected in full scan mode from *m/z* 50–1000 for positive and *m/z* 50–1100 for negative ionization mode. The capillary voltage was set to 3 kV for both ionization modes; the drying gas flow rate was 12 L/min at 250 °C and gas nebulizer 52 psig, fragmentor voltage 175 V for positive and 250 V for negative ionization mode, skimmer 65 V and octopole radio frequency voltage (OCT RF Vpp) 750 V. Data were collected at a rate of 1.0 scan/s. Accurate mass measurements were obtained by means of an automated calibrant delivery system using a Dual Agilent Jet Stream Electrospray ionization (Dual AJS ESI) source that continuously introduces a calibrant solution containing reference masses at *m/z* 121.0509 ($C_5H_4N_4$) and *m/z* 922.0098 ($C_{18}H_{18}O_6N_3P_3F_{24}$) for positive and *m/z* 112.98568 ($C_2O_2F_3(NH_4)$) and 1033.9881 ($C_{18}H_{18}O_6N_3P_3F_{24}$) for negative ionization mode. Data acquisition was performed with MassHunter Workstation Data Analysis B.05.00 (Agilent Technologies).

For the comparison of samples from high and low myopic patients, QC samples were obtained by pooling aliquots of the biological samples. The analytical sequence always was started with injections of the QC pool, followed by samples in a randomized order with a QC injected after each block of 5 samples.

1.5. Data treatment

All data obtained after CE–MS or LC–MS analysis were treated in the same way. Before reprocessing, an initial qualitative analysis was performed to check all the electropherograms/chromatograms in order to detect possible outliers due to instrumental errors.

Raw data acquired were processed to provide structured data in an appropriate format for data analysis. By the use of the Molecular Feature Extraction (MFE) tool in MassHunter Qualitative Analysis software B.06.00 (Agilent Technologies), data collected by CE–MS and LC–MS after each analysis was cleaned of background noise and unrelated ions. The algorithm of the MFE tool groups ions by isotopic distribution, charge-state envelope and/or by the presence of adducts and/or loss of neutral molecule and dimers to generate a list of all the possible components (features). To find co-eluting adducts of the same feature the following adduct settings were applied; for CE–MS and LC–MS in positive ionization mode: $[M+H]^+$, $[M+Na]^+$ and $[M+K]^+$ and for negative ionization mode $[M-H]^-$, $[M-Cl]^-$ and $[M-HCOO]^-$. The possibility of neutral loss of water was also included in each case. Each compound was described by mass, migration time (MT) (CE–MS) or retention time (RT) (LC–MS) and abundance.

Alignment was performed with Mass Profiler Professional software B.05.00 (Agilent Technologies) considering similarities between *m/z* and MT/RT within the samples. The maximum MT shift allowance was set at 2.0 min for CE–MS (maximum shift from the peaks of the internal standard observed in the whole set of electropherograms obtained in the same sequence of analysis) and 0.5 min for LC–MS and a window mass tolerance, in both cases, of 2.0 mDa.

Data were filtered based on a previously optimized strategy known as QA+ [12], whereby variables were retained if they were present in at least 80% of the QCs or absent in QCs, present in 80% of one of the two groups and present with a QC relative standard deviation (RSD) below 30%. In order to reduce the effect of analytical drift observed in the CE–MS analysis, robust LOESS (locally estimated scatter-plot smoothing) signal correction (QC-RLSC) was applied [13]. This procedure was applied in between the QC filters: based on presence and CV.

Multivariate analyses were performed using SIMCA-P+ 12.0 (Umetrics, Umea, Sweden). In order to explore the metabolic features differentiating patients based on exhibiting high or low myopia, orthogonal partial least squares – discriminant analysis (OPLS-DA) was performed. From this, variable importance projection scores (VIP) were generated. OPLS-DA models were validated by leave 1/3 out cross-validation. First a randomized data set was prepared, from which 1/3 of the samples was removed and with the remaining samples (2/3), a new model was built. Then, the excluded samples were predicted by the new models. This process was repeated until every sample has been predicted at least once. For each set of samples predicted, the percentage of correctly classified samples was calculated.

In addition to multivariate analysis, the percentage difference in mean abundance between high and low myopia groups was calculated for each metabolic feature. Those metabolic features with percentage differences between groups > 20 % and with a percentage difference greater than QC RSD by at least 10 % were considered as candidate markers.

1.6. Compound identification

Identification of compounds from CE–MS or LC–MS that were found to be significant in class separation was performed by searching each accurate mass *m/z* against online databases such as METLIN (http://metlin.scripps.edu), KEGG (http://www.genome.jp/kegg/genome.html), HMDB (http://hmdb.ca) and LIPIDMAPS (http://www.lipidmaps.org/). Identification of *m/z* was performed considering each of the possible adducts as described for MFE. Besides that, for CE–MS, compound identification was confirmed by comparing mass and MT to those of an in-house database of standards.

2. Results and discussion

The study consisted of the following experiments: (i) the study of the metabolic profile by CE–MS, whereby six independent preparations were obtained from a sample coming from a healthy individual and (ii) application of metabolomics to study patients with high or low myopia in order to gain insight into the mechanism of the condition through CE–MS and LC–MS.

Please cite this article in press as: C. Barbas-Bernardos, et al., Looking into aqueous humor through metabolomics spectacles – exploring its metabolic characteristics in relation to myopia, J. Pharm. Biomed. Anal. (2016), http://dx.doi.org/10.1016/j.jpba.2016.03.032

2.1. Characterization of the profile

Due to the fact that the nature of the samples is aqueous, characterization of AH was performed with CE–MS, since it enables the detection of the type of compounds expected to be found in AH (aqueous, polar and ionic).

A total of 44 metabolites were identified in human AH following filtration. Putative identifications for each are listed in Table 1 (ordered by their accurate masses). Compounds that were justified by comparison to our in-house standards database are marked with an asterisk. All metabolites could be a consequence of AH being responsible for the supply of nutrients and oxygen to the avascular tissues through diffusion. More than 65 % of the compounds analyzed were amino acids, among which 17 are proteogenic ones (underlined in Table 1), and analogues. Other metabolites were amines (creatine), quinolines (isoquinolines and debrisoquine) fatty acid conjugates (acetylcarnitine, nervonyl carnitine) and two hydrolysis products of glutathione as L-cysteinylglycine disulfide and S-glutathionyl-L- cysteine were found. Moreover, some non-physiological compounds or drugs were identified (lidocaine, phenylephrine, tetracaine, tropisetron, benoxinate. . .) which could be related to the eye treatments. Benoxinate, tetracaine and lidocaine are local anesthetics commonly used in ophthalmology and phenylephrine and tropisetron are mydriatic drugs used to dilate the pupil.

Up to now there have been no other non-targeted metabolomics analyses of human AH samples studied in relation to myopia. Although, AH has been profiled through NMR based metabolomic approaches previously [9,10]. Comparing the profile to those reported for murine models, some of the same compounds were observed. For example, alanine, valine and leucine/isoleucine were detected in both of the previously published articles, while choline and arginine were additionally reported by Song et al. (2011) and proline, creatine glutamine and glutamic acid by Mayordomo-Febrer et al. (2015). Regarding the characterization of the profile, some compounds were previously described for this type of sample, mainly amino acids and other nitrogen containing compounds. For example alanine, creatine, glutamine and valine that were found in this study have also been observed in human AH using high resolution ^{1}H NMR [14]. These together with cysteine and tyrosine have also been observed in AH analyzed by HPLC [15]. In that study, the authors aimed to identify five major low molecular weight water soluble electrochemically active molecules in the AH of three mammalian species. HPLC enabled them to detect also ascorbic acid, and uric acid, two molecules that cannot be easily detected by CE–MS under normal polarity as these analytes migrate towards the negative electrode or cathode.

Many of the features summarized in the characterization (Table 1) are related to methylation processes (methylthioguanine, methylxanthosine, methylhistidine, Nε-methyllysine). This process involves S-adenosylmethionine (SAM) as a main character, a molecule responsible for the donation of methyl groups to proteins, nucleic acids, carbohydrates, lipids and small molecules. Through this donation SAM becomes S-adenosylhomocysteine (SAH), which in a cyclic process becomes SAM again. SAH breaks into adenosine and homocysteine. This homocysteine has various destinies: becoming tetrahydrofolate, becoming methionine which with a molecule of ATP forms SAM, or becomes a precursor of cysteine who at the same time is a precursor for glutathione.

Acylcarnitines are related to tissues that use fatty acids as a source of energy. Carnitines and soluble acylcarnitines were detected in rabbit and camel eyes [16], and with this experiment, it is shown that they are also relevant in human eye.

Additionally, some of the amino acids profiled (phenylalanine, leucine, isoleucine, valine, alanine and threonine) were previously reported as important markers of extreme myopia and senile cataract in AH, measured using an amino acid analyzer [17].

2.2. Metabolomic study with patients with high and low myopia

The results acquired from the metabolomics experiment are based on the analysis of 36 samples (12 with high and 24 with low myopia) and the same samples for LC–MS, except one high myopia sample that was not analyzed.

OPLS-DA analysis was used for modelling the differences between groups. All models showed clear separation of samples (Fig. 1). The parameters of obtained models were satisfied with good quality of variance explained (R^2) and variance predicted (Q^2). Cross-validation, as described in the materials and methods, was used to estimate the predictive ability of the OPLS-DA models based on the filtered data matrix. For data recorded in CE–MS, samples were classified correctly with a rate of 75.93 %, for LC−MS samples were classified correctly with a rate of 96.88 % and 94.79 % for positive and negative ionization mode respectively. Volcano plots were generated by plotting p(corr) against VIP generated from the OPLS-DA model and were used to visualize the statistical significance. VIP scores represent estimates of the importance of each variable in the model. Values close to or greater than one can be considered important in a given model (when combined with p(corr)). In CE–MS the limit was set to VIP > 1 and in LC–MS VIP > 1.5.

The compounds marked by grey squares (Fig. 1 B, D and F) represent those metabolic features contributing most to the model; metabolic features were determined to be significant when they exhibited a VIP score > 1 in addition to presenting a percentage difference between groups more than 20 % and a percentage difference greater than QC RSD by at least 10 %. These features were selected for identification as described in the materials and methods.

Identified metabolites from both CE–MS and from LC–MS (positive and negative ionization modes) are summarized in Table 2, including all the putative assignations, with their experimental accurate *m/z*, MT/RT and their chemical formula. In total, 5 compounds were discovered and biologically interpreted for CE–MS while 15 in LC–MS positive ionization mode and 2 appeared to be significant in LC–MS negative ionization mode. One metabolite (aminoundecanoic acid) was identified in the CE–MS analysis of high and low myopia samples that was not observed in the profile. This is particularly interesting since it could be a specific metabolic signature of myopia and does not compose AH of a healthy eye (or at least in a detectable abundance).

Numerous pieces of evidence show that oxidative stress plays a role in both the progress of myopia and appearance of eye diseases associated [18]. Hence, oxidative damage related to hypoxic myopia can modify the neuromodulation that nitric oxide and dopamine have in eye growth. Moreover, radical superoxide or peroxynitrite production may damage retina, vitreous, lens. . . contributing to the appearance of retinopathies, retinal detachment, cataracts . . . [18]. Arginine and citrulline are two compounds that appeared in the profile and also seem to be relevant in myopia since both were significantly higher in samples from patients with high myopia. These two metabolites are related to each other through nitric oxide synthase (NOS) that catalyzes the formation of NO from arginine in the citrulline-NO cycle [19]. Citrulline and to some extent, one of its stable by-products NG-hydroxy-L-arginine (HOArg), are formed during this reaction and used to quantify the activity of the enzyme. Hattenbach et al. performed a comparison of AH samples from diabetic patients with and without diabetic retinopathy and controls (nondiabetic) using HPLC [19]. Their hypothesis was that the pathway was upregulated resulting in an increase of NO, therefore they studied the concentration of citrulline, arginine and HOArg. The three compounds were detected both in diabetic and nondiabetic patients but HOArg appeared in

Please cite this article in press as: C. Barbas-Bernardos, et al., Looking into aqueous humor through metabolomics spectacles – exploring its metabolic characteristics in relation to myopia, J. Pharm. Biomed. Anal. (2016), http://dx.doi.org/10.1016/j.jpba.2016.03.032

Table 1
List of compounds present in AH and found by CE–MS analysis. Compounds that were justified by comparison to our in-house standards database are marked with an asterisk. All experimental *m/z* reported correspond to $[M+H]^+$ adducts. Proteogenic amino acids are underlined.

Experimental *m/z*	MT (min)	Chemical formula	ID	Class
90.0554	13.41	C3H7NO2	Alanine*	Amino acids, peptides, and analogues
102.1275	11.60	C6H16N	Nervonyl carnitine	Quaternary ammonium salts
104.1071	10.46	C5H14NO	Choline*	Cholines
106.0500	14.54	C3H7NO3	Serine*	Amino acids, peptides, and analogues
116.0710	15.62	C5H9NO2	Proline*	Amino acids, peptides, and analogues
118.0861	14.55	C5H11NO2	Valine*	Amino acids, peptides, and analogues
118.0861	16.33	C5H11NO2	Betaine*	Amino acids, peptides, and analogues
120.0653	15.14	C4H9NO3	Threonine*	Amino acids, peptides, and analogues
130.0858	16.29	C6H11NO2	Pipecolic acid*	Amino acids, peptides, and analogues
130.0862	10.76	C9H7N	Isoquinoline	Isoquinolines and derivatives
132.0767	13.12	C4H9N3O2	Creatine*	Amino acids, peptides, and analogues
132.1018	14.83	C6H13NO2	Leucine/Isoleucine*	Amino acids, peptides, and analogues
133.0611	15.15	C4H8N2O3	Asparagine*	Amino acids, peptides, and analogues
133.0970	10.68	C5H12N2O2	Ornithine*	Amino acids, peptides, and analogues
136.0427	16.77	C4H9NO2S	Homocysteine*	Amino acids, peptides, and analogues
147.0764	15.42	C5H10N2O3	Glutamine*	Amino acids, peptides, and analogues
147.1127	10.76	C6H14N2O2	Lysine*	Amino acids, peptides, and analogues
148.0603	15.42	C5H9NO4	Glutamic acid*	Amino acids, peptides, and analogues
150.0582	15.33	C5H11NO2S	Methionine*	Amino acids, peptides, and analogues
156.0766	11.28	C6H9N3O2	Histidine*	Amino acids, peptides, and analogues
160.1335	12.45	C8H17NO2	Aminooctanoic acid	Amino acids, peptides, and analogues
161.1286	11.02	C7H16N2O2	Nε-methyllysine	Amino acids, peptides, and analogues
162.1123	12.59	C7H15NO3	Carnitine*	Fatty acids and conjugates
166.0870	15.72	C9H11NO2	Phenylalanine*	Phenylpropanoic acids
168.1019	13.12	C9H13NO2	Methoxytyramine	Phenols and derivatives
170.0927	11.52	C7H11N3O2	Methylhistidine*	Amino acids, peptides, and analogues
175.1189	11.06	C6H14N4O2	Arginine*	Amino acids, peptides, and analogues
176.1067	15.71	C6H13N3O3	Citrulline*	Amino acids, peptides, and analogues
176.1180	8.26	C10H13N3	Debrisoquine	Tetrahydroisoquinolines
182.0482	16.75	C6H7N5S	Methylthioguanine	Purine
182.0810	16.02	C9H11NO3	Tyrosine*	Phenylpropanoic acids
188.0709	15.59	C11H9NO2	Indoleacrylic acid	Indoles
203.1484	11.95	C8H18N4O2	asym- dimethylarginine	Amino acids, peptides, and analogues
204.1229	13.20	C9H17NO4	Acetylcarnitine*	Fatty acid esters
205.0970	15.60	C11H12N2O2	Tryptophan*	Indolyl carboxylic acids and derivatives
218.1387	13.50	C10H19NO4	Propionylcarnitine	Fatty acid esters
241.0310	15.89	C6H12N2O4S2	Cystine*	Amino acids, peptides, and analogues
255.1358	6.75	C12H18N2O4	Furosine	Amino acids, peptides, and analogues
276.1185	17.75	C10H17N3O6	N-Succinyl-L-citrulline// Ala Ala Asp/Ala Gly Glu/Gln Glu	Amino acids, peptides, and analogues
298.0522	14.00	C8H15N3O5S2	Cysteinylglycine disulfide	Amino acids, peptides, and analogues
299.0978	9.05	C11H14N4O6	Methylxanthosine	Xanthosines
350.2071	15.87	C18H27N3O4	Ile Ala Phe/Phe Ala Leu	Amino acids, peptides, and analogues
362.1653	11.10	C13H23N5O7	Gln Asn Thr/Gln Gln Ser	Amino acids, peptides, and analogues
427.0947	16.51	C13H22N4O8S2	S-Glutathionyl-L-cysteine	Amino acids, peptides, and analogues

higher concentrations in diabetics suggesting the possibility of NO as a significant factor in the control of retinal vascular functions and changes in diabetes mellitus. Moreover they proposed the production of NO as a potential therapeutic approach for retinopathies related to diabetes.

Another enzyme of the citrulline-NO pathway that has gained importance during the last decades is argininosuccinate synthase (ASS). ASS was first related to the liver [20], where it catalyzes the formation of argininosuccinate, from the condensation of citrulline with aspartate. Argininosuccinate is the precursor of arginine which at the same time leads to urea in the urea cycle. This enzyme was detected in the eyes of rats as well as in other tissues [21], demonstrating its ubiquity and giving rise to the belief that its expression is dependent on the tissue needs (not like in the liver where it is continuously expressed). Koshiyama et al. (2000) also showed that arginine recycling activity from citrulline was present in ocular tissues [21].

Many of the significant differences between high and low myopia were in amino acids. Funding et al. (2005) performed a proteomic analysis of the AH composition to identify the possible mechanism in myopia development since they knew that the expression profile for some proteins in AH, changes within diseases [8]. They stated that the proteins they had identified could play a potential role in the axial elongation occurring in myopia. Many other studies have been published relating AH and proteins [5,6,22,23]. Several peptides were also putatively identified that could be candidates for understanding the metabolic changes in this disease. This could be due to a hydrolysis of the proteins or higher activity of the eye gland.

A relevant difference between high and low myopia was in didehydro-retinoic acid. Eye growth is locally regulated by the retina which detects the sign of defocus to accelerate or reduce axial eye growth. Major retinal signals include dopamine, glucagon (in chick), acetylcholine, NO and retinoic acid [24]. Retinoic acid mediates the growth and development function of vitamin A by acting as a diffusible signaling molecule that modulates the activity of a family of retinoic acid receptors [25]. Hence, retinoic acid has been involved in the signaling cascade that controls eye growth between the retina and the sclera [26,27]. In chicks the changes in ocular growth showed in induced myopia are directly associated with changes in proteoglycan synthesis and proteoglycan accumulation in the sclera at the posterior pole of the eye [28]. Therefore, different studies in animal models [28,29] suggest that choroidal synthesis of all trans retinoic acid in response to visual stimuli can control scleral proteoglycan synthesis.

Please cite this article in press as: C. Barbas-Bernardos, et al., Looking into aqueous humor through metabolomics spectacles – exploring its metabolic characteristics in relation to myopia, J. Pharm. Biomed. Anal. (2016), http://dx.doi.org/10.1016/j.jpba.2016.03.032

Table 2
List of compounds present in AH and found to be statistically significant according to the differences between high and low myopic patients by CE–MS and LC–MS analyses. Positive values in% change represent those higher in low myopia, while negative values represent those higher in high myopia.

Experimental *m/z*	MT/RT (min)	Chemical formula	ID	Adduct	Mass error (ppm)	Analytical technique	% change	VIP
126.0908	0.30	C7H13NO2	Aminocyclohexanecarboxylic acid	$[M+H-H2O]^+$	8	LC–MS (+)	127	2.02
160.1332	11.20/0.26	C8H17NO2	Aminooctanoic acid	$[M+H]^+$	0	CE–MS/LC–MS (+)	−60/-43	2.33/2.07
175.119	9.88	C6H14N4O2	L-Arginine	$[M+H]^+$	0	CE–MS	−23	1.21
176.1033	14.08	C6H13N3O3	Citrulline	$[M+H]^+$	2	CE–MS	−22	1.07
202.1799	12.13	C11H23NO2	Aminoundecanoic acid	$[M+H]^+$	0	CE–MS	230	2.34
213.1463	3.65	C12H22O4	Dodecanedioic acid	$[M+H-H2O]^+$	12	LC–MS (+)	59	2.04
232.1534	0.28	C11H21NO4	Butyryl-L-carnitine	$[M+H]^+$	4	LC–MS (+)	−33	1.59
242.0993	0.27	C9H17NO5	Pantothenic Acid (VITAMIN B5)	$[M+Na]^+$	2	LC–MS (+)	−42	2.30
259.0358	4.78	C11H12O5	Trihydroxyphenyl-gamma-valerolactone	$[M+Cl]^-$	8	LC–MS (−)	133	3.54
281.1855	2.55	C20H26O2	Didehydro-Retinoic acid	$[M+H-H2O]^+$	17	LC–MS (+)	486	5.78
284.2940	7.41	C18H39NO2	Sphinganine	$[M+H-H2O]^+$	4	LC–MS (+)	−58	3.25
298.0524	12.51	C8H15N3O5S2	L-Cysteinylglycine disulfide	$[M+H]^+$	0	CE–MS	75	2.32
303.1398	0.28	C15H18N4O3	Histidinyl-Phenylalanine	$[M+H]^+$	17	LC–MS (+)	−49	2.78
313.1006	3.67	C14H14N6O3	Dihydropteroic acid	$[M-H]^-$	15	LC–MS (−)	81	3.03
352.2451	3.38	C18H35NO4	Dimethylnonanoyl carnitine	$[M+Na]^+$	2	LC–MS (+)	111	2.25
716.5501	7.03	C40H78NO7P	PC(O-32:2)//PC(P-32:1)	$[M+H]^+$	12	LC–MS (+)	−32	1.53
844.6376	8.64	C50H88NO8P	PC (42:6)	$[M+H-H2O]^+$	18	LC–MS (+)	46	2.08
892.6533	6.99	C48H93NO11S	C24 Sulfatide	$[M+H]^+$	0	LC–MS (+)	−35	2.05
		C50H96NO7P	PC(P-42:2)//PC(O-42:3)	$[M+K]^+$	2			
970.7019	8.22	C52H101NO13	LacCer(d40:0)	$[M+Na]^+$	15	LC–MS (+)	−24	1.53
1032.7039	6.67	C54H99NO18	Trihexosylceramide (d36:2)	$[M+H-H2O]^+$	19	LC–MS (+)	45	2.21
1129.8105	6.93	C61H112N2O16	NeuAcaGalCer(d42:2)	$[M+H]^+$	1	LC–MS (+)	27	1.59

Please cite this article in press as: C. Barbas-Bernardos, et al., Looking into aqueous humor through metabolomics spectacles – exploring its metabolic characteristics in relation to myopia, J. Pharm. Biomed. Anal. (2016), http://dx.doi.org/10.1016/j.jpba.2016.03.032

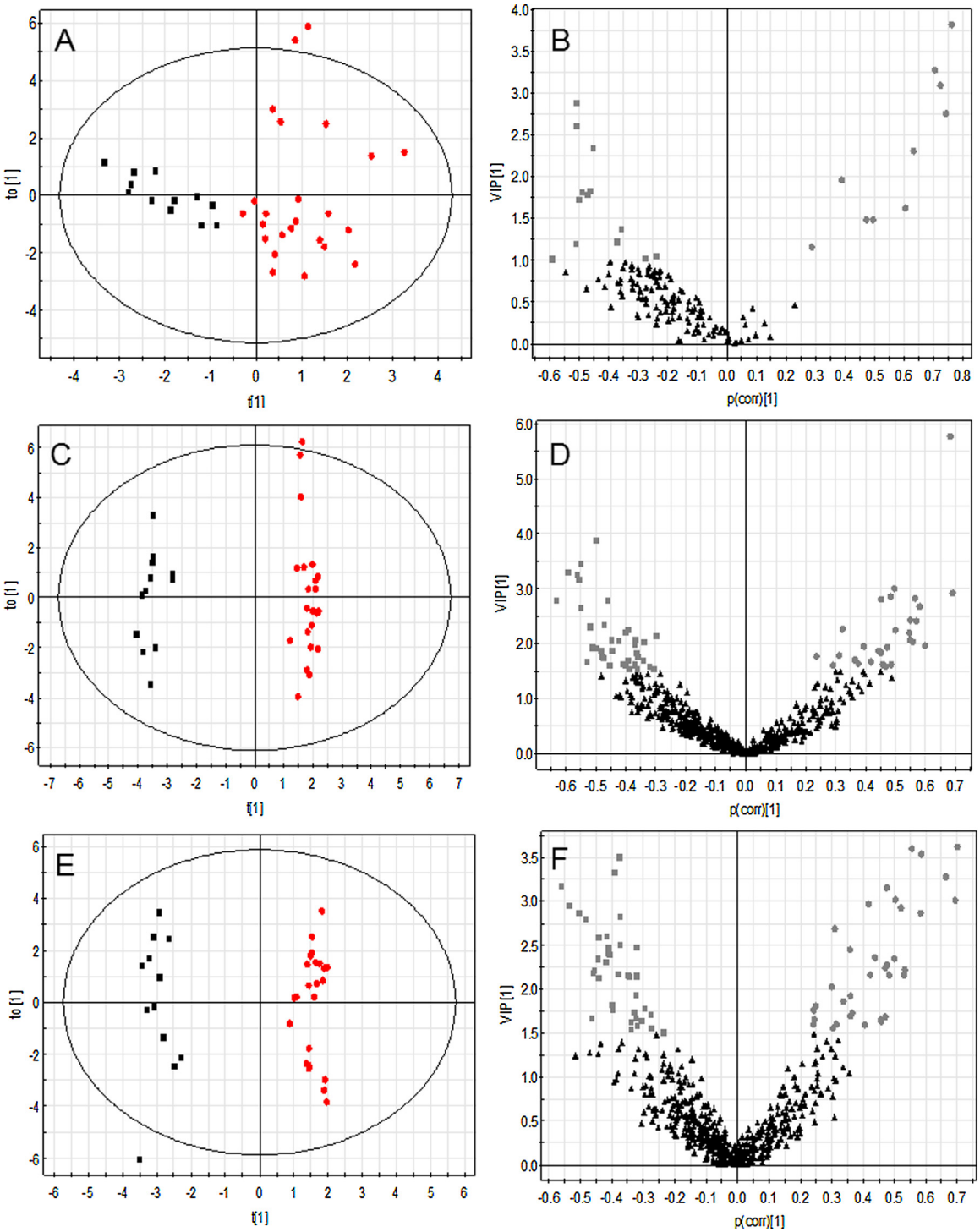

Fig. 1. OPLS-DA models with Log transformation and Pareto scaling for: CE–MS (A) $R^2Y = 0.746$, $Q^2 = 0.517$; LC–MS+ (C) $R^2Y = 0.986$, $Q^2 = 0.824$; and LC–MS- (E) $R^2Y = 0.979$, $Q^2 = 0.673$. Black squares represent samples from patients with high myopia and red dots from those with low myopia. Volcano plots for: CE–MS (B), LC–MS+ (D) and LC–MS- (F). Metabolic features with VIP scores greater than the chosen cut-off are highlighted by grey squares (increased in high myopia) and grey dots (increased in low myopia). (For interpretation of the references to color in this figure legend, the reader is referred to the web version of this article).

A range of lipids were observed that appear to characterize the severity of myopia, one main class of which was sphingolipids. An alteration of sphingolipids and glycosphingolipids metabolism can cause several retinal diseases like Farber's disease, Tay-Sachs/Sandhoff, Gaucher's, Krabbe's and Niemann Pick, diseases often associated to blindness [30] . This shows the importance of sphingolipid metabolism in retinal cells and might explain their appearance in this study.

3. Conclusion

A total of 44 compounds have been putatively identified and characterized by their MT and accurate mass in AH through CE–MS. With the use of a simple method, that requires little sample treatment; polar and ionic compounds have been found by a metabolic fingerprinting approach. Most of them were amino acids derivatives.

Please cite this article in press as: C. Barbas-Bernardos, et al., Looking into aqueous humor through metabolomics spectacles – exploring its metabolic characteristics in relation to myopia, J. Pharm. Biomed. Anal. (2016), http://dx.doi.org/10.1016/j.jpba.2016.03.032

AH samples from myopic patients were also analyzed with two techniques in a mass spectrometry based non-targeted metabolomic study for the first time. A relationship between the general profile and the statistically significant metabolites of the samples from myopic patients was searched by comparing the results obtained with both CEkMS and LC–MS experiments. With CE–MS five compounds were significant and putatively identified. Three appeared to be in higher abundance in high myopia samples (aminooctanoic acid, arginine and citrulline,) while two were less abundant with respect to low myopia samples (aminoundecanoic acid and cysteinylglycine disulfide). The fact that these compounds were identified means they are differentially expressed, in physiological conditions, in the biofluid. This could be because some of them were reabsorbed or because they were produced at a different rate. In LC–MS negative ionization mode two features (trihydroxyphenyl-gamma-valerolactone and dihydropteroic acid) appeared to be statistically significant and putatively identified. The two are in higher concentration in low myopia samples than in high myopia ones. In positive mode 15 features were significant and putatively identified. From these, eight were higher in high myopia and the rest were higher in low myopia. The combined use of CE–MS and LC–MS to analyze AH proves to be highly useful in providing complementary information on the metabolome; only one metabolite was observed by both techniques.

This study provides a comprehensive list of metabolites which may be considered as a reference to look for alterations in their presence in different pathologic conditions of the eye, and offers the opportunity to identify novel biomarkers for each disease and maybe, targets for new therapeutic treatments. All these data allow us to conclude that a metabolomics approach is a powerful tool for profiling of metabolites and drugs in clinical samples.

Acknowledgements

CBB acknowledges her fellowship to USP-CEU. Authors acknowledge funding from the Spanish Ministry of Science and Technology CTQ2014-55279-R and Generalitat Valenciana APM-05/15 in addition to PRCEU-UCH CON-15/05 (CEU – Banco Santander) de Francisco Bosch-Morell and APM-05/15 (Generalitat Valencia) de Amparo Navea.

Appendix A. Supplementary data

Supplementary data associated with this article can be found, in the online version, at http://dx.doi.org/10.1016/j.jpba.2016.03.032.

References

[1] L. Yu, Z.-K. Li, J.-R. Gao, J.-R. Liu, C.-T. Xu, Int. J. Ophthalmol. 4 (2011) 658.
[2] M. Mihelčič, Coll. Antropol. 37 (2013) 251–255.
[3] M. Goel, R.G. Picciani, R.K. Lee, S.K. Bhattacharya, Open Ophthalmol. J. 4 (2010) 52.
[4] G. Barber, Invest. Ophthalmol. 7 (1968) 564.
[5] U.R. Chowdhury, B.J. Madden, M.C. Charlesworth, M.P. Fautsch, Invest. Ophthalmol. Visual Sci. 51 (2010) 4921.
[6] X. Duan, Q. Lu, P. Xue, H. Zhang, Z. Dong, F. Yang, N. Wang, Mol. Vision 14 (2008) 370.
[7] K. Kapnisis, M. Van Doormaal, C.R. Ethier, J. Biomech. 42 (2009) 2454–2457.
[8] M. Funding, H. Vorum, B. Honore, E. Nexø, N. Ehlers, Acta Ophthalmol. Scand. 83 (2005) 31–39.
[9] Z. Song, H. Gao, H. Liu, X. Sun, Curr. Eye Res. 36 (2011) 563–570.
[10] A. Mayordomo-Febrer, M. Lopez-Murcia, J. Morales-Tatay, D. Monleon-Salvado, M. Pinazo-Duran, Exp. Eye Res. 131 (2015) 84–92.
[11] E.G. Armitage, F.J. Rupérez, C. Barbas, TrAC Trends in Anal. Chem. 52 (2013) 61–73.
[12] J. Godzien, V. Alonso-Herranz, C. Barbas, E.G. Armitage, Metabolomics 11 (2014) 518–528.
[13] W.B. Dunn, D. Broadhurst, P. Begley, E. Zelena, S. Francis-McIntyre, N. Anderson, M. Brown, J.D. Knowles, A. Halsall, J.N. Haselden, Nat. Protoc. 6 (2011) 1060–1083.
[14] J.C. Brown, P.J. Sadler, D.J. Spalton, S.M. Juul, A.F. Macleod, P.H. Sönksen, Exp. Eye Res. 42 (1986) 357–362.
[15] S.P. Richer, R. Rose, Vision Res. 38 (1998) 2881–2888.
[16] P. Pessotto, P. Valeri, E. Arrigoni-Martelli, J. Ocul. Pharmacol. Ther. 10 (1994) 643–651.
[17] J. Wuu, L. Wen, T. Chuang, G. Chang, Clin. Chem. 34 (1988) 1610–1613.
[18] B.-M. Francisco, M. Salvador, N. Amparo, Oxid. Med. Cell. Longevity 2015 (2015).
[19] L.O. Hattenbach, A. Allers, C. Klais, F. Koch, M. Hecker, Invest. Ophthalmol. Visual Sci. 41 (2000) 213–217.
[20] S. Ratner, B. Petrack, J. Biol. Chem. 191 (1951) 693–705.
[21] Y. Koshiyama, T. Gotoh, K. Miyanaka, T. Kobayashi, A. Negi, M. Mori, Curr. Eye Res. 20 (2000) 313–321.
[22] R.C. Tripathi, C.B. Millard, B.J. Tripathi, Exp. Eye Res. 48 (1989) 117–130.
[23] E. Rohde, A.J. Tomlinson, D. Johnson, S. Naylor, Electrophoresis 19 (1998) 2361–2370.
[24] F. SCHAEFFEL, Acta Ophthalmol. 92 (2014) (0-0).
[25] T.J. Cunningham, G. Duester, Nat. Rev. Mol. Cell Biol. 16 (2015) 110–123.
[26] A.R. Harper, J.A. Summers, Exp. Eye Res. 133 (2015) 100–111.
[27] J.R. MERTZ, J. WALLMAN, Exp. Eye Res. 70 (2000) 519–527.
[28] J.A.S. Rada, L.R. Hollaway, W. Lam, N. Li, J.L. Napoli, Invest. Ophthalmol. Visual Sci. 53 (2012) 1649.
[29] J.A.S. Rada, L.R. Hollaway, Exp. Eye Res. 92 (2011) 394–400.
[30] R.S. Brush, J.-T.A. Tran, K.R. Henry, M.E. McClellan, M.H. Elliott, M.N.A. Mandal, Invest. Ophthalmol. Visual Sci. 51 (2010) 4422.

Please cite this article in press as: C. Barbas-Bernardos, et al., Looking into aqueous humor through metabolomics spectacles – exploring its metabolic characteristics in relation to myopia, J. Pharm. Biomed. Anal. (2016), http://dx.doi.org/10.1016/j.jpba.2016.03.032